HHS Public Access

Author manuscript

Nat Genet. Author manuscript; available in PMC 2013 December 03.

Published in final edited form as:

Nat Genet. ; 44(2): 157–164. doi:10.1038/ng.1039.

A transgenerational impact of siRNA on chromatin: siRNA amplification in *Caenorhabditis elegans* generates a homology-targeted footprint of H3K9 methylated nucleosomes

Sam Guoping Gu[1], **Julia Pak**[1], **Shouhong Guang**[4,5], **Jay M. Maniar**[2], **Scott Kennedy**[5], and **Andrew Fire**[1,2,3]

[1]Department of Pathology, Stanford University School of Medicine, Stanford, California, 94305, USA.

[2]Department of Genetics, Stanford University School of Medicine, Stanford, California, 94305, USA.

[5]Laboratory of Genetics, University of Wisconsin, Madison, Wisconsin, 53706, USA.

Abstract

Exogenous double-stranded RNA (dsRNA) has been shown to exert homology-dependent effects at the level of both target mRNA stability and chromatin structure. Using *C. elegans* undergoing RNAi as an animal model, we have investigated the generality, scope, and longevity of chromatin-targeted dsRNA effects and their dependence on components of the RNAi machinery. Using high-resolution genome-wide chromatin profiling, we found that a diverse set of genes can be induced to acquire locus-specific enrichment of H3K9 trimethylation, with modification footprints extending several kilobases from the site of dsRNA homology and with locus specificity sufficient to distinguish the targeted locus from among all 20,000 genes in the *C. elegans* genome. Genetic analysis of the response indicated that factors responsible for secondary siRNA production during RNAi were required for effective targeting of chromatin. Temporal analysis revealed that H3K9 methylation, once triggered by dsRNA, can be maintained in the absence of dsRNA for at least two generations before being lost. These results implicate dsRNA-triggered chromatin modification in *C. elegans* as a programmable and locus-specific response defining a metastable state that can persist through generational boundaries.

[3]Corresponding author. Phone: Fax: (650) 724-9070, afire@stanford.edu.

[4]Present Address: School of Life Sciences, University of Science & Technology of China, Hefei, 230026, China.

Data deposit: All sequencing data used in this study were deposited at NCBI GEO database (accession number: GSE32631).

Authors' contribution: Experiments were conceived in discussions amongst all authors. Experiments and data analyses for Fig. 1 were performed by S. Gu, J Pak, J Manniar, S Guang, and S Kennedy, and A Fire. Experiments and data analyses for Fig. 2–5 were performed by S Gu S, J Pak, and A Fire. Overall discussions of data and implications involved all authors, and manuscript was written by Gu S and Fire A.

Introduction

RNA interference (RNAi) is defined by an ability of exogenous double-stranded RNA (dsRNA) to silence homologous target genes [1,2]. The RNAi pathway begins with dsRNA being diced into small RNAs of 20–30 nucleotides (called small interfering RNA, or siRNA) by the RNase III-like enzyme dicer [3]. siRNAs are loaded into highly conserved argonaute proteins, defined by the PIWI and PAZ domains [4]. Target mRNAs, recognized by base-pairing interactions mediated by siRNAs, can then be degraded by a nuclease activity ('slicer') of some argonautes [5–7]. In plants, fungi, and *C. elegans*, dicer-produced siRNA (named primary siRNA) can also trigger *de novo* synthesis of additional small RNA (called "secondary siRNA") through recruitment of RNA-directed RNA polymerases (RdRPs) that use the mature target mRNA as template [8–10]. Endogenous small RNAs that are antisense to transcripts also exist in a variety of eukaryotic species. These endo-siRNAs modulate a diverse set of cellular processes, *e.g.*, gene regulation, genome surveillance, and chromosome transmission [11–15].

In addition to mRNA degradation, RNA-mediated alterations have also been defined at the DNA or chromatin levels [16,17]. This process has been termed "RNA-triggered chromatin modification", as distinguished from cytoplasmic RNA-triggered mRNA degradation mechanisms, referred to as RNAi. RNA-triggered chromatin modification was initially discovered in plants, where it was found that transgene or viral RNA can trigger a local peak of DNA methylation around the target sequence [reviewed in [18,19]]. RNA-mediated DNA methylation in plants involves small RNAs and requires dicer, argonaute, and RdRP family members. In *Schizosaccharomyces pombe*, endogenous small RNAs derived from DNA repeats are associated with heterochromatic gene silencing at the pericentromeric, subtelomeric regions, and the mating type locus [22] [reviewed in [23,24]]. At these heterochromatic loci, RNAi factors (argonaute protein Ago1, dicer protein Dcr1, and RNA-dependent RNA polymerase Rdp1) participate in direct interactions with heterochomatin-associated proteins (*e.g.*, chromodomain protein Chp1), with these interactions required for H3K9 trimethylation (H3K9me3), a histone posttranslational modification associated with silenced chromatin [25–28]. In some cases, exogenous dsRNA was sufficient to direct defined chromatin modification in *S. pombe*[29–32]. An analogous situation may serve as a basis for genome rearrangements during macronuclear development in tetrahymena, where populations of siRNAs have been shown to induce a localized alteration in chromatin that becomes evident on later genome rearrangement[33–35].

Suggestions of siRNA-chromatin associations in animal systems initially came from indirect experiments. One set of observations relate to defects in heterochromatin formation at centromeric regions in *Drosophila* and mouse germ cells affected by mutations in RNAi components [36–38]. While such results outline some type of link between RNA triggers and chromatin modification, the existence of global chromatin defects in mutant strains lacking RNAi components is not prima facie evidence for homology-targeted chromatin modification (rather, some of these defects could be secondary to other major defects in cellular metabolism in the global absence of functional RNA-based regulation). Adding to such debates, different studies in mammalian cell culture have observed a combination of sequence-specific and sequence-nonspecific responses to foreign dsRNA [36–40]. The variety

of results in such assays illustrates both the real potential for diverse responses to siRNA in clinically important systems and the need for model systems to analyze these changes using tractable organisms and genomes [41–43].

Several features make *C. elegans* an attractive animal model to study chromatin-targeted RNA effects. dsRNA can be conveniently introduced to the animals by microinjection, feeding, and soaking [1,44,45], with each mode of administration sufficient to produce substantial effects on target gene expression. A large number of genes can be silenced in *C. elegans*, providing a wide variety of activity assays. *C. elegans* appears to share the ability to respond to dsRNA at both the RNA and chromatin level [46–48]. Early studies in *C. elegans* indicated a reduced level of target mRNA in both the cytoplasm and nucleus of dsRNA-treated embryos [48], with the potential for both specific and non-specific responses at the chromatin level to dsRNA [49]. Recent studies have focused on specific assays for a number of loci, identifying a set of nuclear RNAi defective genes (*e.g.*, *nrde-2* and *nrde-3*) whose functions are required for nucleus-based gene silencing [46,47]. While specificity and generality have been extensively studied for cytoplasmic RNAi, these issues have remained something of a mystery for dsRNA-triggered chromatin modification. In this work, we make use of high-throughput chromatin-structure assays to assess specificity for chromatin-targeted dsRNA effects and characterize the relationship between classical (cytoplasmic) RNAi and RNA-triggered chromatin modification.

Results

Specificity of dsRNA-triggered chromatin modification at the targeted locus

We first examined specificity of dsRNA-triggered H3K9me3 using the target gene *lin-15B*, a model substrate in previous analyses of nuclear effects of RNAi in *C. elegans* [46,47]. A genome-wide assessment of RNAi effects was obtained using chromatin immunoprecipitation (ChIP) of nucleosome core particles[50] followed by high throughput sequencing (Fig. 1). As a number of studies of nuclear RNAi have used *eri-1(mg366)* as a dsRNA-recipient strain ['eri'='enhanced RNAi; [51]], we carried out our initial analysis in synchronized embryos of this genetic background.

An initial view of target specificity was provided by comparing degree of H3K9me3 for each gene under conditions of RNA interference for *lin-15B* with that of control animals (Fig. 1a). Counts from nucleosome cores isolated with H3K9me3 immunoprecipitation were normalized using counts from nucleosome cores isolated without immunoprecipitation. Among the 20,937 *C. elegans* genes surveyed for this analysis, *lin-15B* shows the highest increase in the dsRNA-triggered H3K9me3. Two genes (*lin-15A* and *ZK662.5*) that are located next to *lin-15B* in the genome also show increased H3K9me3 level in the *lin-15B* RNAi sample. Most of the other genes remained distributed along the diagonal line in the scatter plot, indicating little if any change in H3K9 trimethylation in those targets following *lin-15B* RNAi. Another view of target specificity was provided by comparing degree of H3K9me3 for the entire × chromosome (using a 2 Kb smoothing window) under conditions of RNA interference for *lin-15B* and in control animals (Fig. 1b). The biggest difference occurred at the *lin-15B* region (5.7-fold enrichment). These data indicate that that strong

H3K9me3 enhancement following *lin-15B* RNAi was specific to the *lin-15B* region and neighboring loci.

A detailed local analysis evidenced the degree of spreading in the eventual distribution of H3K9me3 following dsRNA administration (Fig. 1c). The highest H3K9me3 level appeared in the trigger region and the flanking region (*e.g.*, on average, H3K9me3 level at the trigger region is 3.7 times of the background-level). Using a cutoff of two-fold changes above the background H3K9me3 level, we found that H3K9me3 can spread as far as 9 kb from the trigger region.

Many *C. elegans* genes are susceptible to dsRNA-triggered chromatin modification

We chose three other target genes (*lir-1*, *ego-1*, and *smg-1*) for RNAi in the *eri-1(mg366)* mutant background. Because *lir-1* is abundantly expressed in embryos [52], we induced *lir-1* RNAi in animals and collected embryos for H3K9me3 profiling. Both *smg-1* and *ego-1* function in germline cells (*smg-1* functions in the somatic cells as well) [53,54]. Therefore, for *smg-1* and *ego-1* RNAi experiments, synchronized adult animals were used.

In control animals not exposed to specific RNAi, the *lir-1*, *ego-1*, and *smg-1* loci have very low levels of H3K9me3 (Fig. 1d–f). In the RNAi animals, we observed a dramatic accumulation of H3K9me3, with strong specificity for the target gene in each case (Fig. 1d–f). These data suggest that many genes in *C. elegans* are susceptible to the dsRNA-triggered chromatin modification.

As with *lin-15B*, we observed a distinctive spatial pattern of dsRNA-triggered chromatin modification for the target loci tested. In each case, the highest levels of H3K9me3 accumulation occurred at the trigger region or immediate flanking regions (Fig. 1d–f). (The H3K9me3 profiles within the trigger regions were excluded for the *smg-1* and *ego-1* RNAi experiments due to DNA fragments from RNAi feeding plasmids that were captured and amplified in IP material. Embryos were devoid of contaminating feeding vector DNA due to a hypochlorite washing step [55] that removes bacteria during embryo preparation). With a cutoff of two-fold changes above the background H3K9me3 level, we found that the H3K9me3 modification can spread as far as 11, 6, and 8 kb from the trigger regions of *lir-1*, *ego-1*, and *smg-1*, respectively. In all cases, the H3K9me3 spread into intergenic regions and some of the neighboring genes. These data indicate that, as a common feature, dsRNA-triggered chromatin modification can spread over a distance from the trigger region equivalent to several genes.

dsRNA-triggering of localized H3K9 trimethylation in the absence of sensitizing mutations

Guang *et al*. have shown that enhanced RNAi mutations in a genetic background is required for some targets in the efficient induction of RNAi phenotypes through nuclear pathways [47]. Similarly, effective chromatin responses to exogenous dsRNA in *S. pombe* have been reported in a subset of studies (see[29,30]) to require mutations in analogous genes.

To test whether sensitizing mutations in the *eri* pathway were required for the chromatin response, we compared H3K9me3 in *eri-1(mg366)* and wild type genetic backgrounds. This analysis was carried out using the target locus *smg-1*. In these experiments, we observed a

positive H3K9me3 response at the target gene in the wild type animals (Fig. 2a), with only a modest decrease in either the degree of observed enrichment in H3K9me3 or extent of RNAi spreading, in comparison with the result from *eri-1* genetic backgrounds. As a control to ensure the ability to detect defects in dsRNA-triggered H3K9me3 in this assay, we measured modification in a *nrde-2(gg091)* genetic background, previously shown to compromise chromatin targeted RNAi. *nrde-2* mutant animals showed a 6-fold loss in H3K9me3 response to dsRNA compared to *eri-1* and wild type strains, demonstrating the specificity of the ChIP-seq assay (Fig. 2a). These data indicate that the chromatin response is not dependent on the *eri-1* mutation. Similar results were obtained for the RNA-enhancing mutation *rrf-3(pk1426)* (Fig. 2b).

The chromatin response is determined by processes on a sub-genic scale

To investigate the relationship between the dsRNA trigger and position of dsRNA-triggered chromatin modification, we examined the effect of a *smg-1* RNAi trigger targeting the 3'UTR (Fig. 2c). We found that this 7-kb downstream shift in the trigger was accompanied by a 7-kp shift in the H3K9me3 peak center (compare Fig. 2a to Fig. 2c). The spatial correlation between the triggering dsRNA and H3K9me3 profile evidences a mechanism in which the specificity of the chromatin response is determined by events on a sub-genic scale.

No methylation signal was observed using dsRNA targeting a region that is upstream to the annotated *smg-1* 5' UTR (Fig. 2c). This observation was consistent with models in which interactions with a pool of target mRNA might play an essential role in eventual targeting of chromatin. As noted below, several other observations support this type of model.

Argonaute requirements indicate a critical role for secondary siRNA accumulation in dsRNA-triggered chromatin modification

Primary and secondary siRNAs in *C. elegans* are two classes of small RNAs that differ in their biogenesis, chemical structure at the 5' end, and strand-specificity. Primary siRNAs are cleaved from the initial dsRNA trigger by dicer, derive from both strands, and carry a 5' monophosphate terminus. Secondary siRNAs are produced through the primary-siRNA guided action of RNA-directed RNA polymerases on specific mRNA templates, resulting in production of large numbers of short antisense transcripts that retain a triphosphate on their 5' end. Two groups of argonaute proteins participate in classical RNAi in *C. elegans*: RDE-1 incorporates primary siRNAs and mediates interactions of the primary siRNAs with target templates, resulting in recruitment of the RdRP activities [9,10,56,57]; a group of additional argonautes (PIWI-1, SAGO-1, SAGO-2, and F58G1.1) then interact with secondary siRNAs, presumably allowing additional target mRNAs to be detected and cleared [57].

To investigate the participation of different small RNA classes and their corresponding argonuate factors in chromatin-targeted RNAi, we examined small RNA profiles and argonaute genetic requirements for this process.

smg-1-targeted RNAi experiments were carried out in populations of *C. elegans* mutant for either *rde-1* [*rde-1(ne300)*] or the secondary argonaute group [MAGO *(ppw-1(tm914),*

sago-1(tm1195), sago-2(tm894), F58G1.1(tm1019), C06A1.4(tm887), and M03D4.6(tm1144)]. Neither population of mutant animals showed above-background H3K9me3 accumulation at the target locus (Fig. 2d), suggesting that the two sets of argonautes are both essential to the dsRNA-triggered chromatin response.

In order to correlate chromatin responses with small RNA populations, we also examined the small RNA profiles in the RNAi worms using a 5'-mono phosphate-independent small RNA cloning method, which captures both the primary (5' monophosphate) and the secondary (5' triphosphate) siRNA. RNAi in the wild type sample produced a large number of small RNAs. In *rde-1(ne300)* and MAGO mutants, the numbers of primary siRNAs at the trigger region were only reduced by 3–4 fold, in comparison with the wild type background (Fig. 3b, c, and d). In contrast, secondary siRNAs levels at the *smg-1* locus in *rde-1(ne300)* and MAGO mutants were reduced by 360 and 197 fold, respectively, as compared with wild type animals (Fig. 3f, g, and h).

Secondary siRNA accumulation alone did not appear to be sufficient for a robust chromosomal effect following *smg-1* RNAi. At least one additional mechanistic requirement in the process was evident from observations that *nrde-2(gg091)* mutant animals, which lack a chromatin-targeted H3K9me3 response, retained their ability to make secondary as well as primary siRNAs (Fig. 3e and i). Somewhat surprisingly, siRNA counts in *nrde-2(gg091)* appeared to be higher than in wild type animals; this could indicate a global readjustment of specific small RNA dynamics in *nrde-2(gg091)* (*e.g.*, an increased *in vivo* stability of siRNAs incorporated into alternative argonautes).

These data are consistent with a mechanism for dsRNA-triggered chromatin modification which depends on (but also extends) the dsRNA-triggered secondary siRNA response.

Multi-generational maintenance of RNAi-triggered chromatin modification

Previous studies have demonstrated that dsRNA-triggered gene silencing effects can last for multiple generations in *C. elegans* [58–60]. Such heritable silencing effects could conceivably have been mediated by small RNA-directed or chromatin-based mechanisms (or a combination of effects). Here we investigated whether the heterchromatin state or/and siRNAs at the RNAi target gene can be maintained for subsequent generations in the absence of continued exposure to the initial dsRNA trigger. To address this question, we profiled the H3K9me3 and siRNAs in progeny of *smg-1* RNAi worms for multiple generations (Fig. 4a and **Methods** section). Briefly, wild type adult animals were exposed to *smg-1* RNAi for 2–3 generations, and subsequently bleached to produce a synchronized population, which was again exposed to *smg-1* RNAi. Adult animals were harvested (P0). Afterwards, we removed the RNAi source and collected F1, F2, and F3 populations at the adult stage for small RNA and H3K9me3 profiling. We observed that the magnitude and spread of the H3K9me3 in the F1 animals were at levels similar to ones in the P0 animals (Fig. 4b). Interestingly, the siRNAs level in the F1 adult animals was much lower than in P0 worms that had been directly exposed to *smg-1* dsRNA (414 and 700 fold depletion for primary and secondary siRNAs, respectively) (Fig. 4d and 4h, compared with Fig. 3b and 3f, respectively). The chromatin response weakened in F2 animals, but was still distinctively present (Fig. 4c). In F3 animals, H3K9me3 levels reverted to near-background (Fig. 4c;

H3K9me3 signals at the *smg-1* region [2 Kb regions that flank the trigger site] from P0, F1, F2, and F3 populations were 8.3, 9.2, 3.7, and 1.6 times of the background level seen in *smg-1* RNAi *nrde-2(gg091)* mutant animals). These results indicate that the H3K9me3 response, once established at the RNAi target gene, can persist for at least 2 generations without any further dsRNA exposure. The persistence could reflect either a very potent biological activity of the residual low levels of trigger RNA found after the initial generation or a maintenance of the modified chromatin in the absence of an RNA requirement.

Time lag between the siRNA accumulation and chromatin response

Previous study has shown that exogenous dsRNA-triggered siRNAs could engage in the RNAi pathway within a few hours [48,57]. Here we investigated the time lag between dsRNA exposure and chromatin response. We did two time-course experiments in which worms were harvested 4 or 24 hours after synchronized larvae start to feed on bacteria expressing *smg-1* dsRNA (see Fig. 5a for the scheme). L4 larvae were harvested for each experiment for small RNA and H3K9me3 profiling to provide populations of both somatic and germline tissues. We observed a high level of *smg-1* siRNAs at the 4-hour time point, with even higher *smg-1* siRNA levels at the 24-hour time point (Fig. 5c–f), indicating an ongoing RNAi process. In contrast, we did not observe any accumulation of H3K9me3 at the *smg-1* locus in either the 4 or 24-hour RNAi samples (Fig. 5b). These data indicate that, in addition to be required for H3K9 methylation (see above), siRNA accumulation precedes that of H3K9me3. Moreover, we suggest that distinct and separable mechanisms mediate these events.

Discussion

We have described several features and genetic requirements for the dsRNA-triggered chromatin modification in *C. elegans*, with our results showing that (1) the chromatin response can be highly specific in triggering a window of H3K9me3 surrounding genomic sequences corresponding to a triggering dsRNA, (2) the chromatin response can be targeted to many *C. elegans* genes, (3) secondary-siRNA produced through an initial interaction with an mRNA product are associated with and apparently integral to the chromatin response, (4) in time course experiments, dsRNA-triggered chromatin modification lags behind the initial siRNA response, and (5) chromatin changes can outlast the major small RNA pools, yielding heritable effects. This work differs from a number of important previous studies [41–43,46,47] in that we have demonstrated a direct and highly targeted relationship between the dsRNA sequences introduced into the system and the specific modification of the corresponding chromosomal region. This work draws a clear analogy to well studies RNA-triggered chromatin modification systems originally described in plants [16–18,61] and more recently in fungi [29].

The requirement of *rde-1* and *MAGO* genes for dsRNA-triggered chromatin modification strongly suggests that secondary siRNAs may participate in a connection between cytoplasmic and nuclear dsRNA responses. In particular, primary siRNA production is apparently not sufficient to trigger chromatin modification. The strong spatial correlation between the dsRNA-triggered H3K9me3 and the triggering dsRNA is consistent with a

model in which the secondary siRNAs (likely in an argonaute-dependent manner) directly target the nascent transcript (or even DNA) for chromatin modification.

A role for secondary siRNA machinery in triggering of nuclear events is apparently conserved rather widely, at least in lower eukaryotes. In particular, it is of interest to note the requirement for RdRP homologs in transgene-RNA-directed DNA methylation in Arabidopsis and in site-specific hairpin-induced heterochromatin formation in *S. pombe*[20,21,31,32]. In both cases an initial aberrant RNA trigger appears insufficient for site-specific chromatin modification, requiring the RdRP activity and presumably the resulting secondary siRNAs for alteration at the chromatin level.

Introns near the dsRNA trigger region show high H3K9me3 even though the siRNA levels are low. It is possible that the siRNA-associated chromatin modification enzymes directly act on sites that are somewhat spatially removed from an initial siRNA::transcript interaction. Alternatively, the apparent spreading of the siRNA-induced signal may reflect an ability of H3K9me3 nucleosomes to recruit machinery that enforces new rounds of chromatin modification.

H3K9me3 is associated with repetitive DNA, centromere, and other DNA elements that need to be silenced constitutively. Our multigenerational analysis indicated that the dsRNA-triggered H3K9me3 could be passed onto subsequent generations, suggesting a possible basis for long-term control of mobile elements. Despite heritability of the altered chromatin state for several generations, we found that the chromatin at the target gene eventually reverted to the original (active) state in the absence of the trigger, which is consistent with heritability of small RNAs being finite [58]; this suggests that truly heterochromatic states may need to be maintained by periodic production of an RNA trigger.

A working model for RNA-triggered chromatin modification is shown in Fig. 6. Exogenous dsRNA is first processed by DICER complexes to produce primary siRNAs, which guide RDE-1 to its target mRNA, engaging RdRP activities to copy the target, yielding secondary siRNAs. Secondary siRNAs interact with a dedicated set of argonautes including PPW-1, SGAO-1, SAGO-2, and F58G1.1. These interactions appear to be required for dsRNA-triggered H3K9 methylation. One possibility is that these siRNAs enter the nucleus directly, enforcing chromatin modification through interaction with either the nascent transcript or the DNA template. Alternatively the siRNAs may be synthesized in the nucleus, or may be "handed off" in the cytoplasm to a shuttling argonaute, whose transport into the nucleus would then allow interaction with nascent RNA or DNA. The last model, albeit more complex, is supported by the requirement for NRDE-3 and for the corresponding cytoplasm-to-nucleus transport factor NRDE-2 for effective gene silencing in at least some cases [46,47]. Once secondary siRNA-containing complex recognizes a chromatin-associated target (base pairing with nascent transcripts or DNA), a next step would be the recruitment of a chromatin-modifying complex, producing a localized alteration in histone code including the methylation of H3K9 in nearby nucleosomes. The delayed time course of the chromatin response (compared with the fast siRNA response) suggests that the downstream components of this pathway (entry of small RNAs into the nucleus and/or modification of

histone code) may produce effects that are both slower and more stable than their mRNA-targeted RNAi counterparts.

Methods

C. elegans mutant strains used in this study

C. elegans strain N2 [55] was used as the standard wild-type strain. Mutant alleles used in this study were *eri-1(mg366)* [51], *rde-1(ne300)* [63], *rrf-3(pk1426)* [56], *nrde-2(gg091)* [46], MAGO *(ppw-1(tm914), sago-1(tm1195), sago-2(tm894), F58G1.1(tm1019), C06A1.4(tm887), and M03D4.6(tm1144))*[57], *glp-1(e2141)*[64], and *glp-4(bn2)*[65].

All genomic coordinates are relative to version WS190 (wormbase[66])

RNAi

RNAi by feeding was carried out as previously described [44]. The initial *smg-1* RNAi vector (chrI:6,907,993-6,909,159) was from the Cambridge RNAi library [67]. Other RNAi vectors used in this study were prepared in vector L4440 [68]. The relevant target positions are chrX: 15,728,059-15,728,991 (*lin-15B*), chrII:7,680,827-7,682,011 (*lir-1*), chrI: 7,654,481-7,655,024 (ego-1), chrI:6,901,030-6,901,541 (*smg-1*, 3' end), and chrI: 6,913,664-6,913,933 (*smg-1*, 5' end).

Multigenerational analysis of RNAi response

Wild type adult animals were raised on bacterial producing dsRNA for *smg-1*(chrI: 6,907,993-6,909,159) for 2–3 generations, followed by bleaching to produce a synchronized population [55], and continued culture on smg-1 dsRNA (chrI:6,907,993-6,909,159) bacteria. Adult animals from this population (designated as the "P0" generation for this experiment) were collected and divided into two portions. One portion was used for the siRNA and H3K9me3 profiling. The other portion was bleached to produce progeny designated as the "F1" generation. The bleaching also serves to destroy bacteria expressing the dsRNA, allowing dsRNA triggering to be discontinued in the F1 animals, which were fed on OP50 E. coli lacking a dsRNA-producing plasmid. F2 and F3 animals were similarly raised on OP50 E. Coli. Populations of F1, F2, and F3 animals were then collected as adults for siRNA and H3K9me3 profiling.

H3K9me3 nucleosome immunoprecipitation

50–100 μl frozen embryo pellets or 100 – 200 μl frozen adult worm pellets were used for each nucleosome immunoprecipitation experiment. Crushed pellets (pulverized by grinding in liquid nitrogen with a mortar and pestle) were resuspended in 1 ml buffer A (15 mM Hepes-Na, pH 7.5, 60 mM KCl, 15 mM NaCl, 0.15 mM beta-mecaptoethonal, 0.15 mM spermine, 0.15 mM spermidine, 0.34 M sucrose, 1× HALT protease and phosphatase inhibitor cocktail (Thermo Scientific)). To crosslink, formaldehyde was added to the resulting crude extract to a final concentration of 2%, followed by incubation at room temperature for 15 min. 0.1 ml 1 M Tris.Cl (pH 7.5) was then added to quench formaldehyde. Lysate was spun (15,000×g for 1 min). Pellets were washed with ice-cold buffer A and then resuspended in 0.3 ml buffer A with 2 mM $CaCl_2$. Micrococcal nuclease

(Roche) was added to the lysate to a final concentration of 0.3 U/μl, followed by 5 minutes incubation at 37°C (inverting the tube several times per minute). Micrococcal Nuclease (MNase) digestion was optimized so that approximately 70% of DNA entered the mono-nucleosome band, with the remainder predominantly in di- and trinucleosome bands. Digestion reactions were stopped by adding EGTA to a final concentration of 20 mM. After centrifugation (15,000×g, 1 min) pellets were washed with ice-cold RIPA buffer (1×PBS, 1% NP40, 0.5% Sodium Deoxycholate, 0.1% SDS, 1× HALT protease and phophatase inhibitor and 2 mM EGTA), resuspended in 0.8 ml ice-cold RIPA buffer, and solubilized by sonication (Microson TM XL 2000 sonicating machine with a micro tip, output level: 5, three times of 30-second sonication). Sonication was used here to efficiently solubilize crosslinked chromatin without further fragmenting the chromatin (data not shown). Crude lysate was cleared by centrifugation at 15,000×g for 2 min. 80 μl of the supernatant was used to make "IP input" nucleosome libraries. The remaining supernatant was used for IP, adding 2 μg of anti-H3K9me3 antibody (Abcam, ab8898) and agitating gently at 4°C overnight before 50 μl of protein A Dynabeads (10% slurry in 1× PBS buffer) was added and the resulting mixture shaken for 2hr at 4°C . The beads were then washed four times (four minutes each) with ice-cold 600 μl LiCl washing buffer (100mM Tris.Cl, pH 7.5, 500mM LiCl, 1%NP-40, 1% Sodium deoxycholate), transferring to a new tube after the first wash. To elute the immunoprecipitated nucleosome and reverse crosslinks, beads were incubated with 450 μl worm lysis buffer (0.1M Tris.Cl, pH 8.5, 100 mM NaCl, 1% SDS) containing 200 μg/ml protease K at 65°C for four hours with agitation every 30 minutes (total nucleosome aliquots were treated similarly to reverse crosslink), followed by organic extraction and DNA precipitation. DNA libraries were prepared as previously described [50], with the following change: IP or input DNA was used for end processing linker ligation without size selection. Linkered DNA corresponding to the nucleosome cores was size selected on a 6% denaturing PAGE gel (8 M urea).

High throughput DNA sequencing and data analysis

DNA libraries were sequenced using Illumina GAIIX. After removing barcodes, 25-nt reads were aligned to the *C. elegans* genome (SW190) using Bowtie [69] (see Table 1 for more detailed experimental description). Only perfect alignments were used for analysis. Nucleosome cores were modeled as 147 bases of sequences, extending from the first base of alignment. Nucleosome coverage at any given position was calculated by dividing the number of nucleosome cores that cover this position by the number of total alignments (in millions). If a read matches to multiple places in the genome, a fraction (1/the number of matches) was used to calculate the nucleosome coverage.

Small RNA capture and sequencing

Small RNAs were captured using a 5'-monophosphate-independent method [70] (see Table 1 for more detailed experimental description). To obtain a provisional measure of primary siRNA levels, we doubled the count of sense-stranded siRNAs in the trigger region, avoiding ambiguity in assigning antisense siRNAs in the trigger region by doubling the sense counts. A measure of secondary siRNAs from a given trigger region was then obtained by subtracting half of the presumed primary siRNA counts from total siRNAs on the antisense strand.

Acknowledgements

We thank Ziming Weng, Phil Lacroute, Arend Sidow, Huibin Zhang, Jason Merker, Diane Wu, Karen Artiles, Lia Gracey, Ayelet Lamm, Cecilia Mello, Michael Stadler, Rosa Alcazar, Julie Ni for help, suggestions and support, and the National Institutes of Health (grant R01-GM37706).

Reference

1. Fire A, et al. Potent and specific genetic interference by double-stranded RNA in Caenorhabditis elegans. Nature. 1998; 391:806–811. [PubMed: 9486653]
2. Kennerdell JR, Carthew RW. Use of dsRNA-mediated genetic interference to demonstrate that frizzled and frizzled 2 act in the wingless pathway. Cell. 1998; 95:1017–1026. [PubMed: 9875855]
3. Bernstein E, Caudy AA, Hammond SM, Hannon GJ. Role for a bidentate ribonuclease in the initiation step of RNA interference. Nature. 2001; 409:363–366. [PubMed: 11201747]
4. Hammond SM, Boettcher S, Caudy AA, Kobayashi R, Hannon GJ. Argonaute2, a link between genetic and biochemical analyses of RNAi. Science. 2001; 293:1146–1150. [PubMed: 11498593]
5. Tuschl T, Zamore PD, Lehmann R, Bartel DP, Sharp PA. Targeted mRNA degradation by double-stranded RNA in vitro. Genes Dev. 1999; 13:3191–3197. [PubMed: 10617568]
6. Hammond SM, Bernstein E, Beach D, Hannon GJ. An RNA-directed nuclease mediates post-transcriptional gene silencing in Drosophila cells. Nature. 2000; 404:293–296. [PubMed: 10749213]
7. Elbashir SM, Lendeckel W, Tuschl T. RNA interference is mediated by 21- and 22-nucleotide RNAs. Genes Dev. 2001; 15:188–200. [PubMed: 11157775]
8. Motamedi MR, et al. Two RNAi complexes, RITS and RDRC, physically interact and localize to noncoding centromeric RNAs. Cell. 2004; 119:789–802. [PubMed: 15607976]
9. Pak J, Fire A. Distinct populations of primary and secondary effectors during RNAi in C. elegans. Science. 2007; 315:241–244. [PubMed: 17124291]
10. Sijen T, Steiner FA, Thijssen KL, Plasterk RH. Secondary siRNAs result from unprimed RNA synthesis and form a distinct class. Science. 2007; 315:244–247. [PubMed: 17158288]
11. Saito K, Siomi MC. Small RNA-mediated quiescence of transposable elements in animals. Dev Cell. 19:687–697. [PubMed: 21074719]
12. Claycomb JM, et al. The Argonaute CSR-1 and its 22G-RNA cofactors are required for holocentric chromosome segregation. Cell. 2009; 139:123–134. [PubMed: 19804758]
13. Batista PJ, et al. PRG-1 and 21U-RNAs interact to form the piRNA complex required for fertility in C. elegans. Mol Cell. 2008; 31:67–78. [PubMed: 18571452]
14. Gent JI, et al. Distinct phases of siRNA synthesis in an endogenous RNAi pathway in C. elegans soma. Mol Cell. 2010; 37:679–689. [PubMed: 20116306]
15. Maniar JM, Fire AZ. EGO-1, a C. elegans RdRP, modulates gene expression via production of mRNA-templated short antisense RNAs. Curr Biol. 2011; 21:449–459. [PubMed: 21396820]
16. Wassenegger M, Heimes S, Riedel L, Sanger HL. RNA-directed de novo methylation of genomic sequences in plants. Cell. 1994; 76:567–576. [PubMed: 8313476]
17. Matzke MA, Primig M, Trnovsky J, Matzke AJ. Reversible methylation and inactivation of marker genes in sequentially transformed tobacco plants. EMBO J. 1989; 8:643–649. [PubMed: 16453872]
18. Wassenegger M. RNA-directed DNA methylation. Plant Mol Biol. 2000; 43:203–220. [PubMed: 10999405]
19. Herr AJ, Baulcombe DC. RNA silencing pathways in plants. Cold Spring Harb Symp Quant Biol. 2004; 69:363–370. [PubMed: 16117669]
20. Dalmay T, Hamilton A, Rudd S, Angell S, Baulcombe DC. An RNA-dependent RNA polymerase gene in Arabidopsis is required for posttranscriptional gene silencing mediated by a transgene but not by a virus. Cell. 2000; 101:543–553. [PubMed: 10850496]
21. Mourrain P, et al. Arabidopsis SGS2 and SGS3 genes are required for posttranscriptional gene silencing and natural virus resistance. Cell. 2000; 101:533–542. [PubMed: 10850495]

22. Volpe TA, et al. Regulation of heterochromatic silencing and histone H3 lysine-9 methylation by RNAi. Science. 2002; 297:1833–1837. [PubMed: 12193640]
23. Grewal SI. RNAi-dependent formation of heterochromatin and its diverse functions. Curr Opin Genet Dev. 20:134–141. [PubMed: 20207534]
24. Moazed D. Small RNAs in transcriptional gene silencing and genome defence. Nature. 2009; 457:413–420. [PubMed: 19158787]
25. Mellone BG, et al. Centromere silencing and function in fission yeast is governed by the amino terminus of histone H3. Curr Biol. 2003; 13:1748–1757. [PubMed: 14561399]
26. Peters AH, et al. Partitioning and plasticity of repressive histone methylation states in mammalian chromatin. Mol Cell. 2003; 12:1577–1589. [PubMed: 14690609]
27. Snowden AW, Gregory PD, Case CC, Pabo CO. Gene-specific targeting of H3K9 methylation is sufficient for initiating repression in vivo. Curr Biol. 2002; 12:2159–2166. [PubMed: 12498693]
28. Bannister AJ, et al. Selective recognition of methylated lysine 9 on histone H3 by the HP1 chromo domain. Nature. 2001; 410:120–124. [PubMed: 11242054]
29. Buhler M, Verdel A, Moazed D. Tethering RITS to a nascent transcript initiates RNAi- and heterochromatin-dependent gene silencing. Cell. 2006; 125:873–886. [PubMed: 16751098]
30. Simmer F, et al. Hairpin RNA induces secondary small interfering RNA synthesis and silencing in trans in fission yeast. EMBO Rep. 2010; 11:112–118. [PubMed: 20062003]
31. Simmer F, et al. Loss of the putative RNA-directed RNA polymerase RRF-3 makes C. elegans hypersensitive to RNAi. Curr Biol. 2002; 12:1317–1319. [PubMed: 12176360]
32. Iida T, Nakayama J, Moazed D. siRNA-mediated heterochromatin establishment requires HP1 and is associated with antisense transcription. Mol Cell. 2008; 31:178–189. [PubMed: 18657501]
33. Aronica L, et al. Study of an RNA helicase implicates small RNA-noncoding RNA interactions in programmed DNA elimination in Tetrahymena. Genes Dev. 2008; 22:2228–2241. [PubMed: 18708581]
34. Malone CD, Anderson AM, Motl JA, Rexer CH, Chalker DL. Germ line transcripts are processed by a Dicer-like protein that is essential for developmentally programmed genome rearrangements of Tetrahymena thermophila. Mol Cell Biol. 2005; 25:9151–9164. [PubMed: 16199890]
35. Nowacki M, et al. RNA-mediated epigenetic programming of a genome-rearrangement pathway. Nature. 2008; 451:153–158. [PubMed: 18046331]
36. Pal-Bhadra M, et al. Heterochromatic silencing and HP1 localization in Drosophila are dependent on the RNAi machinery. Science. 2004; 303:669–672. [PubMed: 14752161]
37. Deshpande G, Calhoun G, Schedl P. Drosophila argonaute-2 is required early in embryogenesis for the assembly of centric/centromeric heterochromatin, nuclear division, nuclear migration, and germ-cell formation. Genes Dev. 2005; 19:1680–1685. [PubMed: 16024657]
38. Kanellopoulou C, et al. Dicer-deficient mouse embryonic stem cells are defective in differentiation and centromeric silencing. Genes Dev. 2005; 19:489–501. [PubMed: 15713842]
39. Taira K. Induction of DNA methylation and gene silencing by short interfering RNAs in human cells (Retraction). Nature. 2006; 441:1176. [PubMed: 16810259]
40. Weinberg MS, Barichievy S, Schaffer L, Han J, Morris KV. An RNA targeted to the HIV-1 LTR promoter modulates indiscriminate off-target gene activation. Nucleic Acids Res. 2007; 35:7303–7312. [PubMed: 17959645]
41. Morris KV, Chan SW, Jacobsen SE, Looney DJ. Small interfering RNA-induced transcriptional gene silencing in human cells. Science. 2004; 305:1289–1292. [PubMed: 15297624]
42. Kim DH, Villeneuve LM, Morris KV, Rossi JJ. Argonaute-1 directs siRNA-mediated transcriptional gene silencing in human cells. Nat Struct Mol Biol. 2006; 13:793–797. [PubMed: 16936726]
43. Weinberg MS, et al. The antisense strand of small interfering RNAs directs histone methylation and transcriptional gene silencing in human cells. RNA. 2006; 12:256–262. [PubMed: 16373483]
44. Timmons L, Fire A. Specific interference by ingested dsRNA. Nature. 1998; 395:854. [PubMed: 9804418]
45. Tabara H, Grishok A, Mello CC. RNAi in C. elegans: soaking in the genome sequence. Science. 1998; 282:430–431. [PubMed: 9841401]

46. Guang S, et al. Small regulatory RNAs inhibit RNA polymerase II during the elongation phase of transcription. Nature. 2010; 465:1097–1101. [PubMed: 20543824]
47. Guang S, et al. An Argonaute transports siRNAs from the cytoplasm to the nucleus. Science. 2008; 321:537–541. [PubMed: 18653886]
48. Montgomery MK, Xu S, Fire A. RNA as a target of double-stranded RNA-mediated genetic interference in Caenorhabditis elegans. Proc Natl Acad Sci U S A. 1998; 95:15502–15507. [PubMed: 9860998]
49. Grishok A, Sinskey JL, Sharp PA. Transcriptional silencing of a transgene by RNAi in the soma of C. elegans. Genes Dev. 2005; 19:683–696. [PubMed: 15741313]
50. Gu SG, Fire A. Partitioning the C. elegans genome by nucleosome modification, occupancy, and positioning. Chromosoma. 2009; 119:73–87. [PubMed: 19705140]
51. Kennedy S, Wang D, Ruvkun G. A conserved siRNA-degrading RNase negatively regulates RNA interference in C. elegans. Nature. 2004; 427:645–649. [PubMed: 14961122]
52. Dufourcq P, et al. lir-2, lir-1 and lin-26 encode a new class of zinc-finger proteins and are organized in two overlapping operons both in Caenorhabditis elegans and in Caenorhabditis briggsae. Genetics. 1999; 152:221–235. [PubMed: 10224256]
53. Smardon A, et al. EGO-1 is related to RNA-directed RNA polymerase and functions in germ-line development and RNA interference in C. elegans. Curr Biol. 2000; 10:169–178. [PubMed: 10704412]
54. Hodgkin J, Papp A, Pulak R, Ambros V, Anderson P. A new kind of informational suppression in the nematode Caenorhabditis elegans. Genetics. 1989; 123:301–313. [PubMed: 2583479]
55. Brenner S. The genetics of Caenorhabditis elegans. Genetics. 1974; 77:71–94. [PubMed: 4366476]
56. Sijen T, et al. On the role of RNA amplification in dsRNA-triggered gene silencing. Cell. 2001; 107:465–476. [PubMed: 11719187]
57. Yigit E, et al. Analysis of the C. elegans Argonaute family reveals that distinct Argonautes act sequentially during RNAi. Cell. 2006; 127:747–757. [PubMed: 17110334]
58. Alcazar RM, Lin R, Fire AZ. Transmission dynamics of heritable silencing induced by double-stranded RNA in Caenorhabditis elegans. Genetics. 2008; 180:1275–1288. [PubMed: 18757930]
59. Grishok A, Tabara H, Mello CC. Genetic requirements for inheritance of RNAi in C. elegans. Science. 2000; 287:2494–2497. [PubMed: 10741970]
60. Vastenhouw NL, et al. Gene expression: long-term gene silencing by RNAi. Nature. 2006; 442:882. [PubMed: 16929289]
61. Hamilton AJ, Baulcombe DC. A species of small antisense RNA in posttranscriptional gene silencing in plants. Science. 1999; 286:950–952. [PubMed: 10542148]
62. Tabara H, Yigit E, Siomi H, Mello CC. The dsRNA binding protein RDE-4 interacts with RDE-1, DCR-1, and a DExH-box helicase to direct RNAi in C. elegans. Cell. 2002; 109:861–871. [PubMed: 12110183]
63. Tabara H, et al. The rde-1 gene, RNA interference, and transposon silencing in C. elegans. Cell. 1999; 99:123–132. [PubMed: 10535731]
64. Austin J, Kimble J. glp-1 is required in the germ line for regulation of the decision between mitosis and meiosis in C. elegans. Cell. 1987; 51:589–599. [PubMed: 3677168]
65. Beanan MJ, Strome S. Characterization of a germ-line proliferation mutation in C. elegans. Development. 1992; 116:755–766. [PubMed: 1289064]
66. Harris TW, et al. WormBase: a comprehensive resource for nematode research. Nucleic Acids Res. 38:D463–D467. [PubMed: 19910365]
67. Kamath RS, et al. Systematic functional analysis of the Caenorhabditis elegans genome using RNAi. Nature. 2003; 421:231–237. [PubMed: 12529635]
68. Timmons L, Court DL, Fire A. Ingestion of bacterially expressed dsRNAs can produce specific and potent genetic interference in Caenorhabditis elegans. Gene. 2001; 263:103–112. [PubMed: 11223248]
69. Langmead B, Trapnell C, Pop M, Salzberg SL. Ultrafast and memory-efficient alignment of short DNA sequences to the human genome. Genome Biol. 2009; 10:R25. [PubMed: 19261174]

70. Gent JI, et al. A Caenorhabditis elegans RNA-directed RNA polymerase in sperm development and endogenous RNA interference. Genetics. 2009; 183:1297–1314. [PubMed: 19805814]

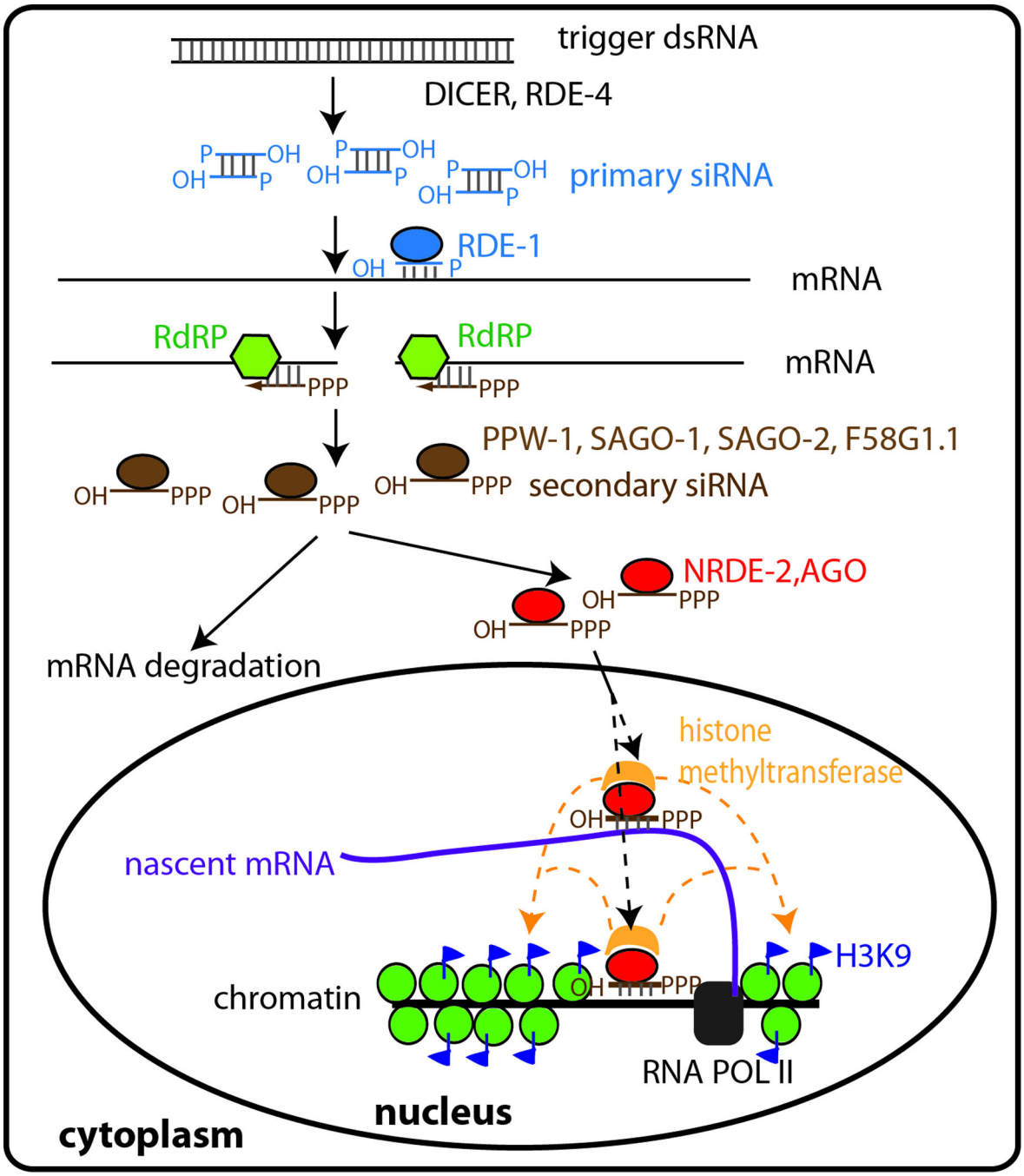

Figure 1.

H3K9me3 profiles triggered by gene-specific dsRNAs. (**a**) A gene-based scatter plot representation of H3K9me3 levels of 20,937 *C. elegans* genes in *lin-15B* RNAi and control (empty vector) samples. Levels of H3K9me3 at each of the 20,937 *C. elegans* genes are presented as a ratio of H3K9me3 nucleosome counts to total nucleosome counts (each normalized to total number of genome-matching counts for the corresponding library). Data points for *lin-15B (purple)* and its two flanking genes, *lin-15A (red)* and ZK662.5 (*green*) are highlighted. The dotted diagonal line reflects unchanged H3K9me3 levels. (**b**) A

position-based plot of H3K9me3 differences between *lin-15B* RNAi and control animals as a function of position on chromosome × provides an assessment of the specificity of chromatin modification on a whole-chromosome scale. (**c–f**) H3K9me3 level as a function of position around *lin-15B* (**c**), *lir-1* (**d**), *ego-1* (**e**), and *smg-1* (**f**) loci. For each of the samples indicted in the legends, H3K9me3 level was calculated as the H3K9me3 nucleosome coverage normalized to total number of genome-matching counts for the corresponding library. dsRNA trigger regions are indicated by orange blocks. For samples derived from adult animals (panels **e** and **f** in this figure), we discard reads to map precisely to the RNAi trigger vector to avoid a background level of DNA deriving from the bacterial food source. No such background was observed in embryonic samples (panels **c** and **d** from this figure) where a Clorox treatment used to prepare embryos removes all traces of bacterial derived DNA.

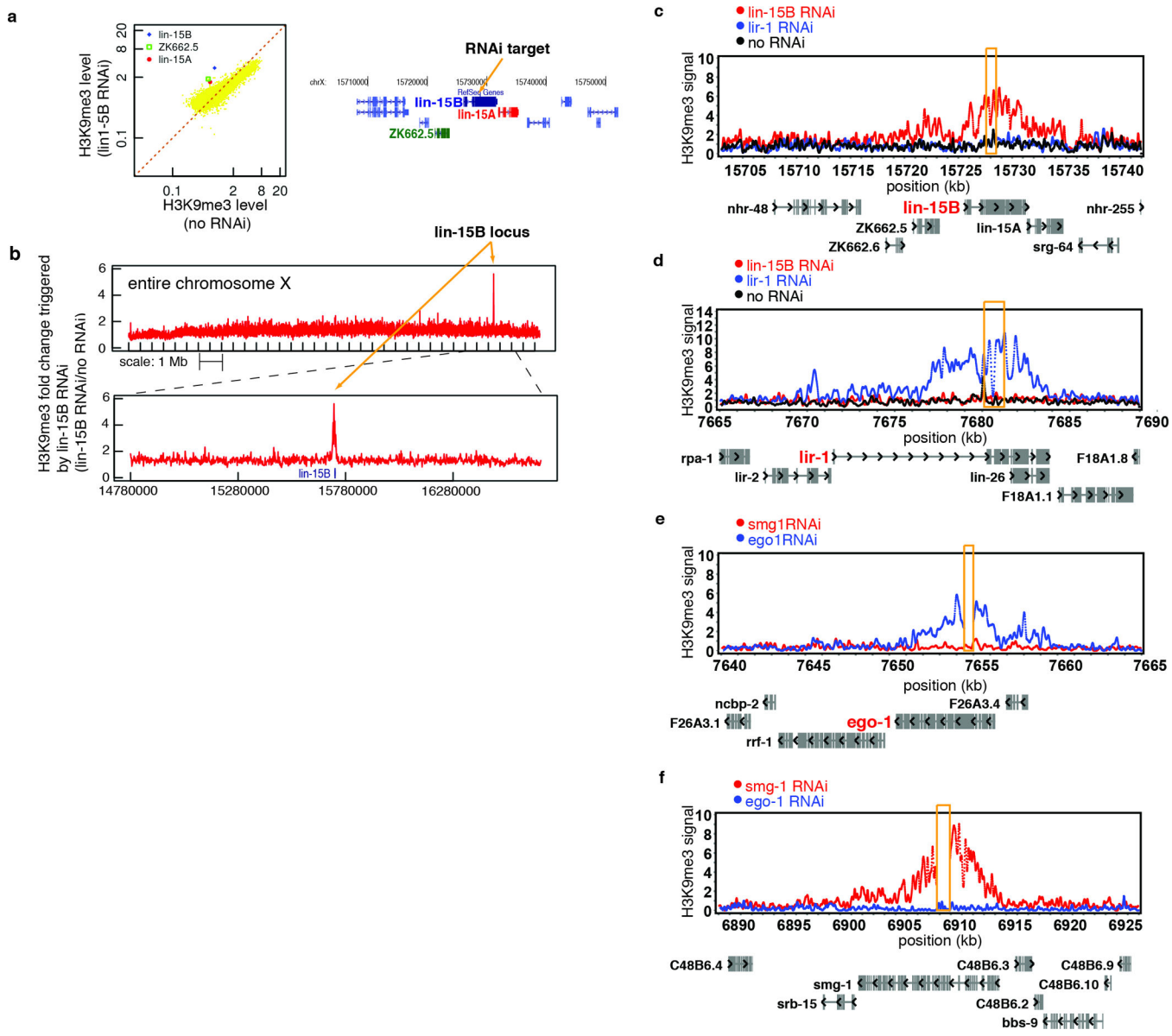

Figure 2.

H3K9me3 profiles triggered by dsRNAs that target different sections of the *smg-1* locus: middle section of *smg-1* (**a, b,** and **d**), 3' UTR of *smg-1* (**c**), and a region that is upstream to the 5' end of *smg-1* mRNA (**c**). Trigger regions are indicated by orange blocks. Genetic backgrounds used in these analyses, were as indicated (wild type N2 strain, *rrf-3*(*pk1426*), *nrde-2*(*gg091*), rde-1(ne300), and MAGO[*ppw-1*(*tm914*), *sago-1*(*tm1195*), *sago-2*(*tm894*), *F58G1.1*(*tm1019*)] mutant strains). The H3K9me3 profile generated from the *nrde-2* mutant (smg-1 RNAi) represents a baseline of H3K9me3 modification in the absence of a functional RNAi pathway. (e) Schematic map of the smg-1 locus.

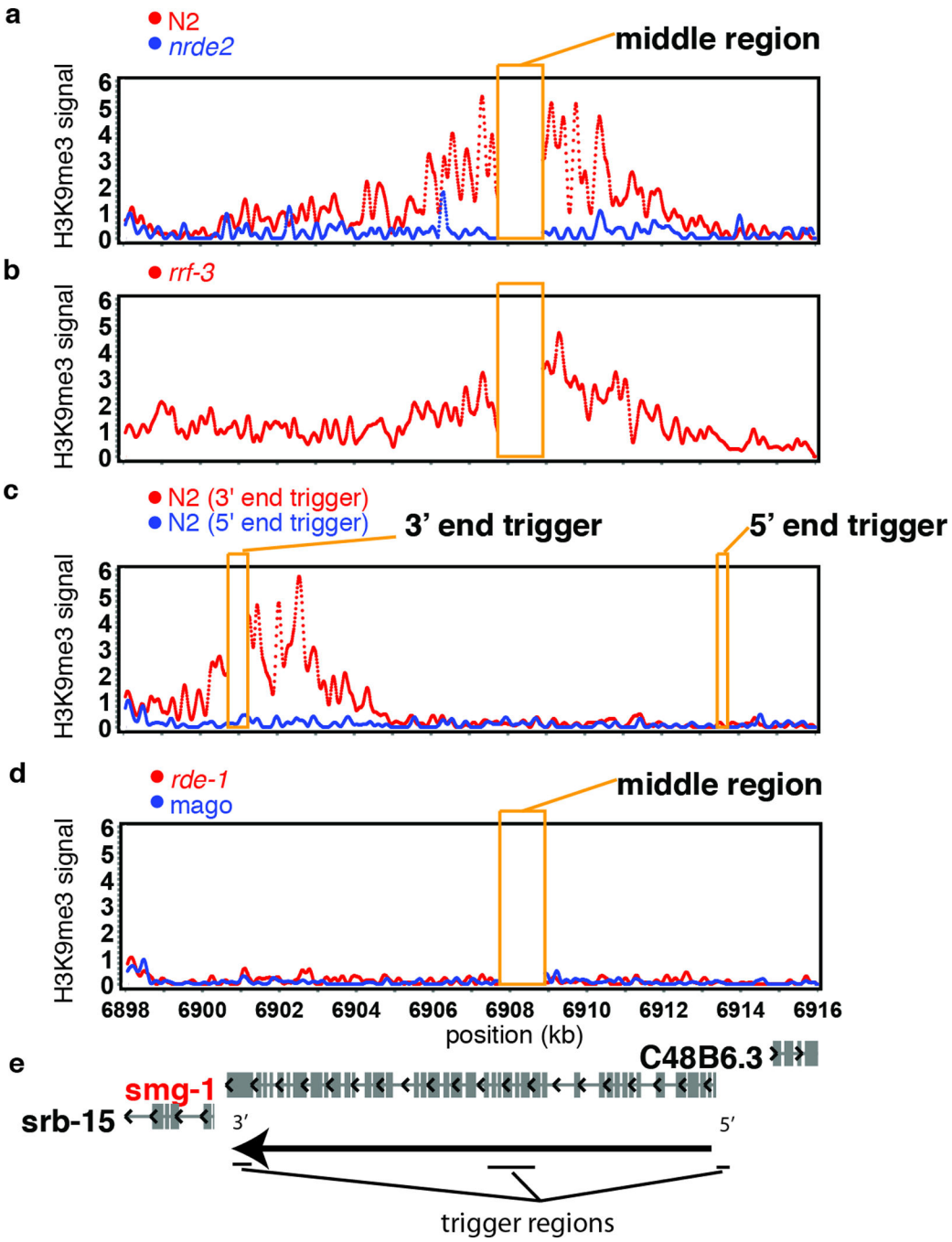

Figure 3.

Small RNA profiles (**b–i**) at *smg-1* locus in wild type (N2), *rde-1*(*ne300*), *nrde-2*(*gg091*), and MAGO[*ppw-1*(*tm914*), *sago-1*(*tm1195*), *sago-2*(*tm894*), *F58G1.1*(*tm1019*), *C06A1.4*(*tm887*), *and M03D4.6*(*tm1144*)] backgrounds. Coverages for small RNAs that matched the smg-1 mRNA-sense strand (**b–e**) or the smg-1 mRNA-antisense strand (**f–i**) were plotted separately. Level of small RNAs was normalized by the total number (in millions) of small RNAs that matched the reverse complementary sequences of total *C. elegans* mRNAs.

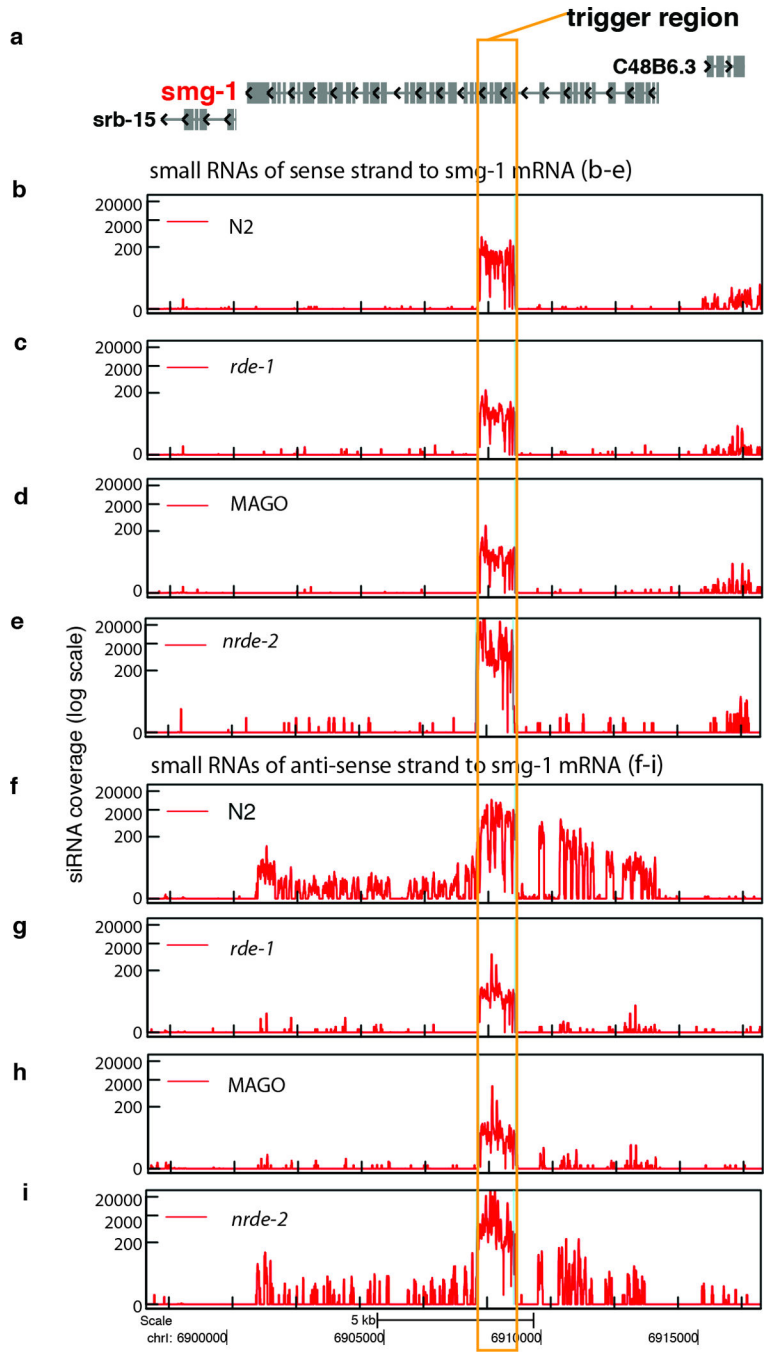

Figure 4.

Multi-generational analyses of H3K9me3 and siRNAs at the RNAi target locus. (**a**) Experimental scheme. (**b–c**) H3K9me3 profiles at *smg-1* locus in animals of different generations. (**d–g**) Coverage levels of small RNAs that matched the smg-1 mRNA-sense strand. (**h–k**) Coverage levels of small RNAs that matched the smg-1 mRNA-antisense strand. For small RNA profiles from “N2 control” (**g** and **k**), wild type N2 adult animals that were undergoing RNAi against a different gene, *sel-1*, were used. As a reference, P0 small RNA levels (from Figure 3b,f) are shown with a dotted line.

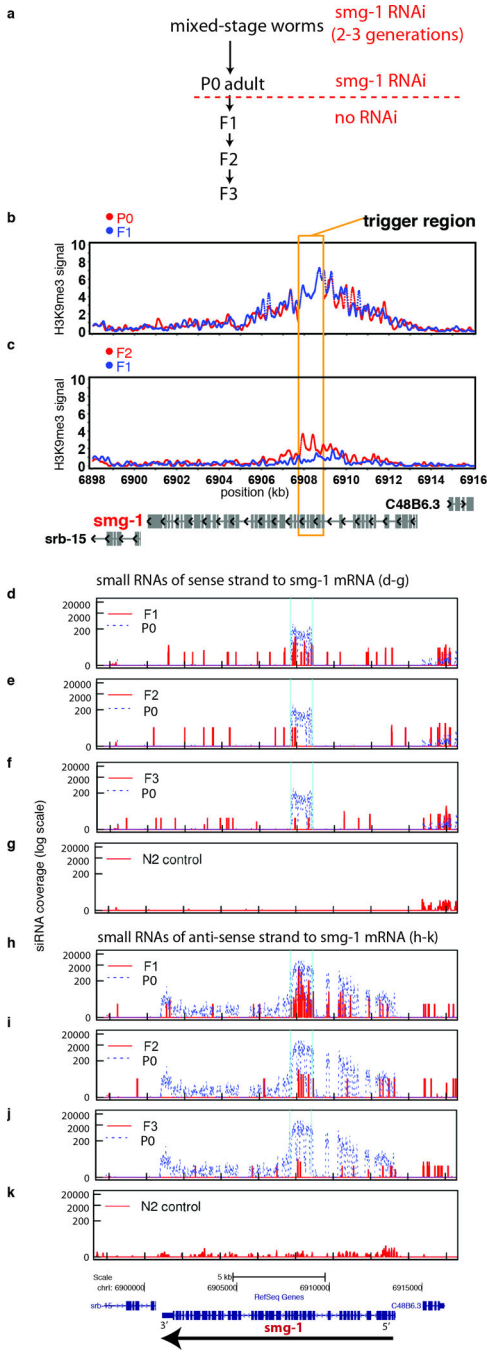

Figure 5.

Time lag between the initial dsRNA exposure and chromatin and siRNA responses. Animals were fed on bacteria expressing *smg-1* dsRNA for different time periods as indicated in the experimental scheme (**a**). (**b**) H3K9me3 profiles at *smg-1* locus. (**c** and **d**) Coverage levels of small RNAs that matched the smg-1 mRNA-sense strand. (**e** and **f**) Coverage levels of small RNAs that matched the smg-1 mRNA-antisense strand.

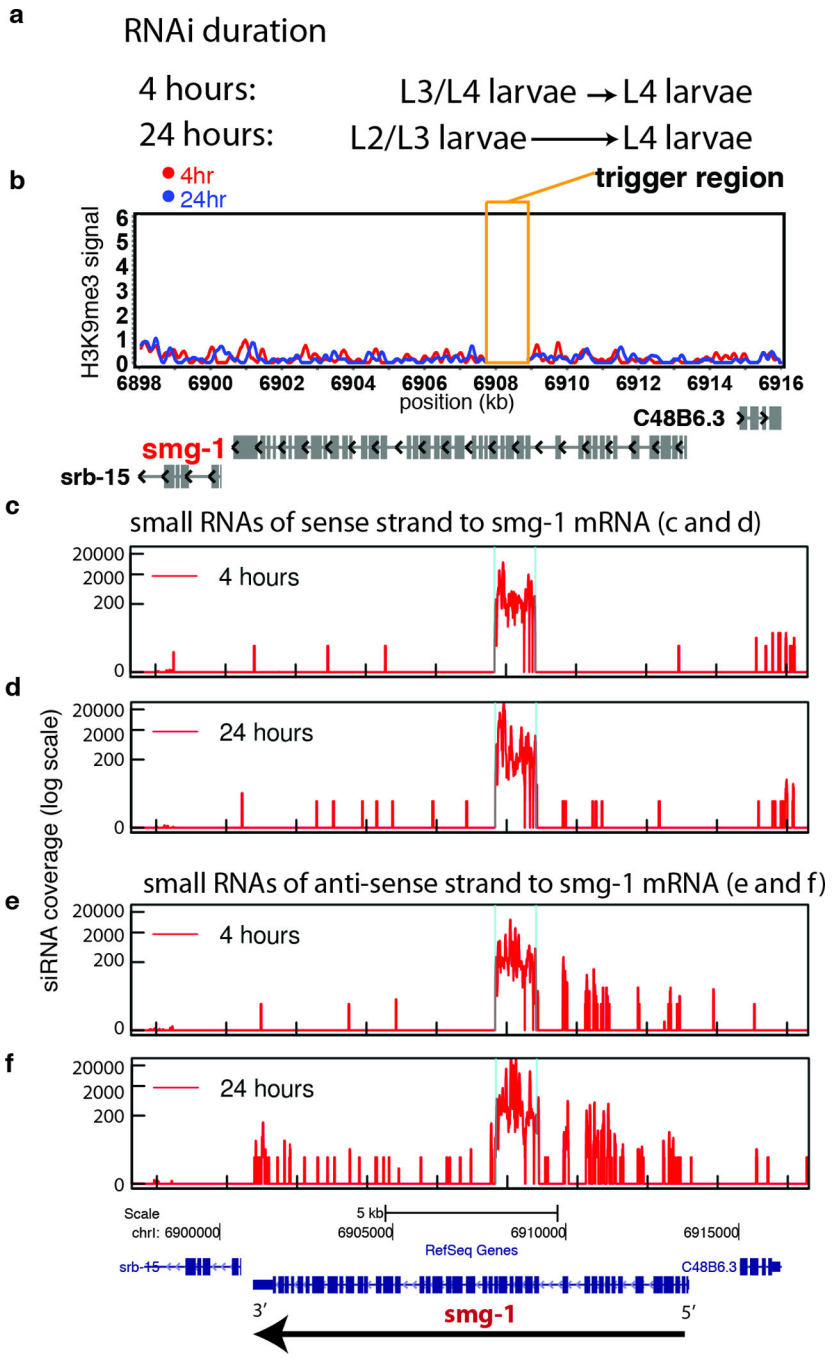

Figure 6.

A working model for dsRNA-triggered H3K9 methylation in *C. elegans*. The dsRNA trigger is digested to primary siRNAs through the activity of Dicer [3] and RDE-4[62]. Primary siRNAs then incorporate into complexes with the RDE-1 argonaute[63], triggering recruitment of RdRP activities (ego-1[53] and rrf-1[56]), secondary siRNAs resulting from RdRP activity then incorporate into complexes with a second group of argonautes[57], including NRDE-2[46]. Targeted binding of siRNA:NRDE-2 complexes to nascent transcripts on the chromosome is proposed (directly or indirectly) to recruit one or more histone modifying components

eventually leading to H3K9 methyltransferase recruitment and the observed H3K9 modification.

Table 1

Description of libraries used for this study.

library name	experiment description	type of library	genetic background	dsRNA target site	number of reads that perfectly match the genome
SG0910_4lib	*ego-1* RNAi	H3K9me3 IP nucleosome	*eri-1 (mg366)*	chrI: 7655024-7654481 (ego-1)	7,458,471
SG0910_6lib	*smg-1* RNAi	H3K9me3 IP nucleosome	*eri-1 (mg366)*	chrI:6,907,993-6,909,159 (smg-1)	11,363,856
V74_7IPmix_CAT	*lin-15B* RNAi	H3K9me3 IP nucleosome	*eri-1 (mg366)*	chrX: 15728059-15728991 (lin-15B)	11,626,719
SG0810_15lib	*lir-1* RNAi	H3K9me3 IP nucleosome	*eri-1 (mg366)*	chrII:7680827-7682011 (lir-1)	22,575,828
V74_7IPmix_ACG	control, no RNAi	H3K9me3 IP nucleosome	*eri-1 (mg366)*		10,275,693
SG0411_lib54	*smg-1* RNAi (targeting the 3'end)	H3K9me3 IP nucleosome	N2	chrI:6,901,030-6,901,541 (smg-1)	7,186,203
SG0411_lib52	*smg-1* RNAi (targeting the 5'end)	H3K9me3 IP nucleosome	N2	chrI:6,913,664-6,913,933 (smg-1)	9,066,039
SG0411_lib20	*smg-1* RNAi	H3K9me3 IP nucleosome	N2	chrI:6,907,993-6,909,159 (smg-1)	7,748,563
SG0411_lib61	*smg-1* RNAi	H3K9me3 IP nucleosome	*nrde-2(gg091)*	chrI:6,907,993-6,909,159 (smg-1)	5,342,704
SG0111_9lib_CAT	*smg-1* RNAi	H3K9me3 IP nucleosome	*rrf-3 (pk1426)*	chrI:6,907,993-6,909,159 (smg-1)	13,550,730
SG0211_24lib	*smg-1* RNAi	H3K9me3 IP nucleosome	*rde-1(ne300)*	chrI:6,907,993-6,909,159 (smg-1)	13,212,520
SG0211_23lib	*smg-1* RNAi	H3K9me3 IP nucleosome	MAGO *(ppw-1(tm914), sago-1(tm1195), sago-2(tm894), F58G1.1(tm1019), C06A1.4(tm887), and M03D4.6(tm1144)*	chrI:6,907,993-6,909,159 (smg-1)	14,629,944
AF_SOL_385	*smg-1* RNAi	small RNA cloning	N2	chrI:6,907,993-6,909,159 (smg-1)	9,344,019
AF_SOL_388	*smg-1* RNAi	small RNA cloning	MAGO *(ppw-1(tm914), sago-1(tm1195), sago-2(tm894), F58G1.1(tm1019), C06A1.4(tm887), and M03D4.6(tm1144)*	chrI:6,907,993-6,909,159 (smg-1)	6,374,634
AF_SOL_389	*smg-1* RNAi	small RNA cloning	*rde-1(ne300)*	chrI:6,907,993-6,909,159 (smg-1)	9,736,340
SG0511_lib1	*smg-1* RNAi	small RNA cloning	*nrde-2(gg091)*	chrI:6,907,993-6,909,159 (smg-1)	9,594,600
SG0411_lib28	P0 of multigenerational experiment	H3K9me3 IP nucleosome	N2	chrI:6,907,993-6,909,159 (smg-1)	6,665,856
SG0411_lib30	F1 of multigenerational experiment	H3K9me3 IP nucleosome	N2		6,404,696
SG0411_lib32	F2 of multigenerational experiment	H3K9me3 IP nucleosome	N2		7,192,377
SG0411_lib34	F3 of multigenerational experiment	H3K9me3 IP nucleosome	N2		7,058,857
SG0411_lib14	24 hours of smg-1 RNAi feeding	H3K9me3 IP nucleosome	N2	chrI:6,907,993-6,909,159 (smg-1)	6,522,036
SG0411_lib16	4 hours of smg-1 RNAi feeding	H3K9me3 IP nucleosome	N2	chrI:6,907,993-6,909,159 (smg-1)	7,342,460
SG0511_lib9	F1 of multigenerational experiment	small RNA cloning	N2		5,994,713
SG0511_lib10	F2 of multigenerational experiment	small RNA cloning	N2		1,892,615

library name	experiment description	type of library	genetic background	dsRNA target site	number of reads that perfectly match the genome
SG0511_lib11	F3 of multigenerational experiment	small RNA cloning	N2		4,591,831
SG0511_lib7	24 hours of *smg-1* RNAi feeding	small RNA cloning	N2	chrI:6,907,993-6,909,159 (smg-1)	5,111,519
SG0511_lib8	4 hours of *smg-1* RNAi feeding	small RNA cloning	N2	chrI:6,907,993-6,909,159 (smg-1)	3,823,974